MOCVD epitaxy of InAlN on different templates*

Yun Lijun(贠利君)†, Wei Tongbo(魏同波), Yan Jianchang(闫建昌), Liu Zhe(刘喆), Wang Junxi(王军喜), and Li Jinmin(李晋闽)

R&D Center for Semiconductor Lighting, Institute of Semiconductors, Chinese Academy of Sciences, Beijing 100083, China

Abstract: InAlN epilayers were grown on high quality GaN and AlN templates with the same growth parameters. Measurement results showed that two samples had the same In content of $\sim$ 16%, while the crystal quality and surface topography of the InAlN epilayer grown on the AlN template, with 282.3″ (002) full width at half maximum (FWHM) of rocking curve, 313.5″ (102) FWHM, surface roughness of 0.39 nm and V-pit density of 2.8×10^8 cm^{-2}, were better than that of the InAlN epilayer grown on the GaN template, 309.3″, 339.1″, 0.593 nm and 4.2×10^8 cm^{-2}. A primary conclusion was proposed that both the crystal quality and the surface topography of the InAlN epilayer grown on the AlN template were better than that of the InAlN epilayer grown on the GaN template. Therefore, the AlN template was a better choice than the GaN template for getting high quality InAlN epilayers.

Key words: InAlN; epilayer; template; crystal quality; surface topography

DOI: 10.1088/1674-4926/32/9/093001 **EEACC:** 4220

1. Introduction

During the past ten years or so, group III-nitride semiconductors, with their wide variation of direct band gap, high thermal and chemical stability[1, 2], have attracted much interest because of their applications, such as semiconductor optoelectronics, through the realization of efficient UV and blue laser diodes (LDs) and light emitting diodes (LEDs)[3], and the fabrication of high power, high frequency electronics; for example, high electron mobility transistors (HEMTs)[4]. However, until recently, fundamental and applied research has essentially focused on AlGaN and InGaN alloys. The $In_xAl_{1-x}N$ alloy is much less well known despite its potentialities, especially that it can be grown perfectly lattice matched to GaN when the indium content is about 17%–18%[5, 6]. The reasons leading to the difficulty in getting high quality InAlN film are as follows. (1) AlN grown at high temperature and low V/III ratio while InN is grown at low temperature and high V/III ratio makes a very narrow growth window and the phenomenon of phase separation and non-uniform component. (2) It's more prone to phase separation and non-uniform component for InAlN, compared with InGaN, due to the large difference in the lattice parameters, bond length and thermal stability of AlN and InN[7]. (3) Atoms on the epitaxial film have low mobility at low growth temperature, especially Al atoms, which makes it difficult to get high quality InAlN film with a flat surface.

Devices based on an InAlN/GaN heterostructure, such as high electron mobility transistors (HEMTs)[8, 9] and distributed Bragg reflectors (DBRs)[5, 10, 11], have been reported in recent years. Nearly lattice matched heterostructures, such as InAlN/GaN, InAlN/InGaN and InAlN/AlGaN, can be used as an active region in LDs and LEDs by regulating the lattice parameters of InAlN to match with other epilayers. In addition, when the In content is about 0.17, InAlN alloy, having a relatively large conduct band offset ((0.9–1.0) $\pm$ 0.3 eV) and small valence band offset (0.2 $\pm$ 0.3 eV)[12], can take the place of AlGaN with 0.2 Al content as the electron blocking layer (EBL) in LEDs[13−15], which can block the electrons coming from the active region more efficiently, enhance recombination efficiency for electrons and holes in the active region and reduce the droop effect, especially in green LEDs at large current. Therefore, how to achieve a high quality InAlN epilayer receives increasing interest and becomes more and more important.

In this work, we have grown InAlN epilayers on GaN

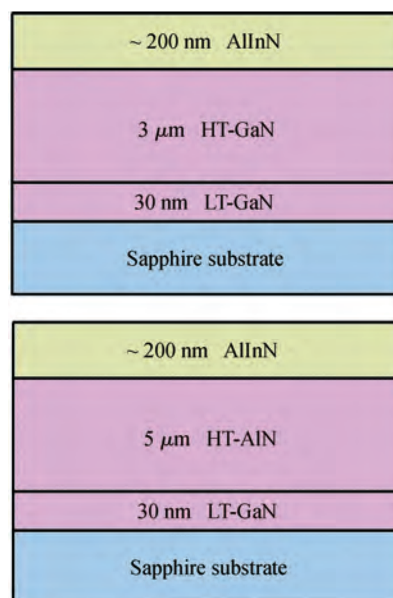

Fig. 1. Schematic diagram of InAlN/GaN and InAlN/AlN heterostructures grown by MOCVD.

* Project supported by the National Natural Science Foundation of China (No. 60806001), the National High Technology Research and Development Program of China (No. 2011AA03A103), and the National Basic Research Program of China (No. 2011CB301904).

† Corresponding author. Email: yunlijun09@gmail.com

Received 7 April 2011, revised manuscript received 5 May 2011

© 2011 Chinese Institute of Electronics

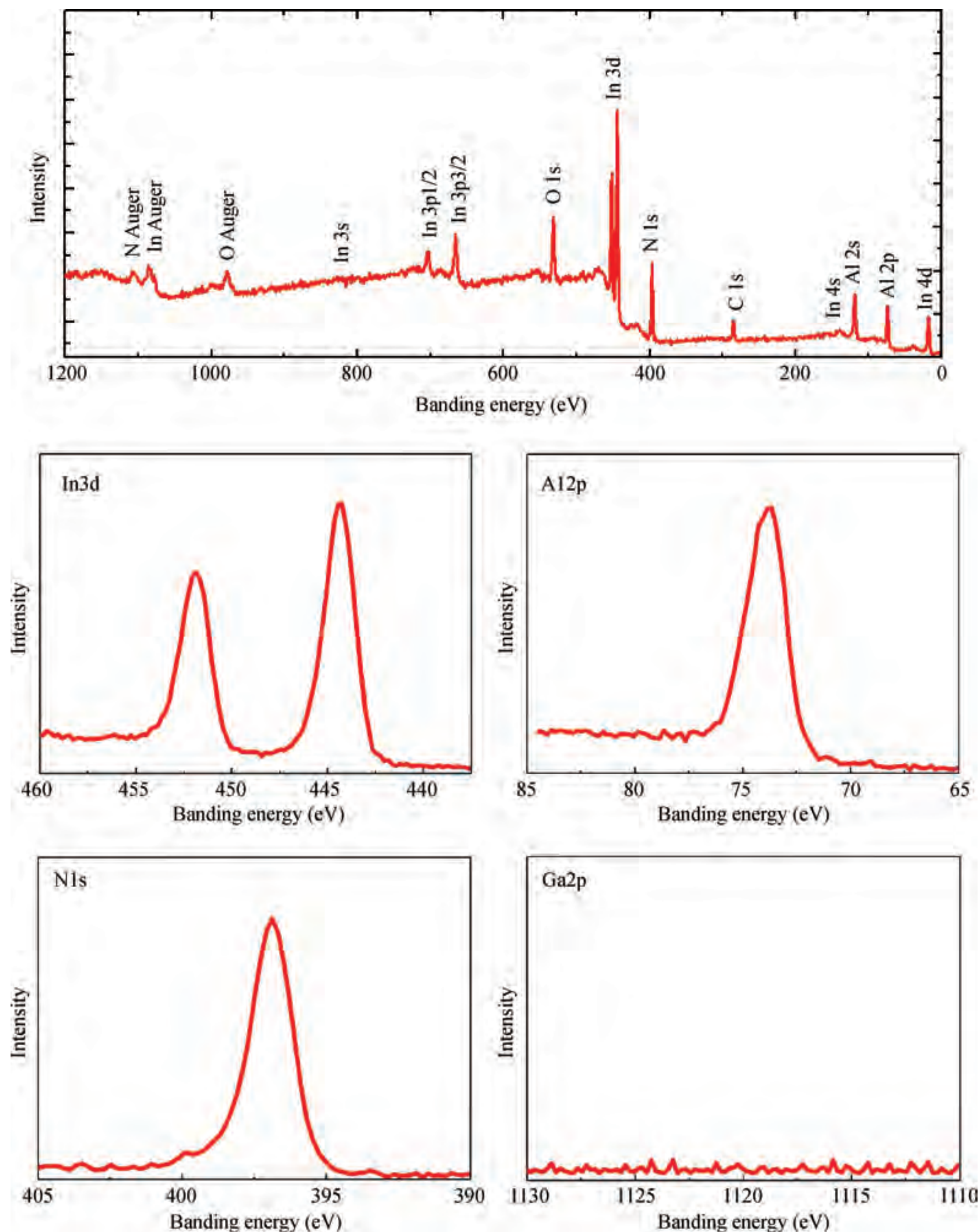

Fig. 2. Near-surface XPS spectra for an InAlN epilayer grown on a GaN template.

and AlN templates by metal organic chemical vapor deposition (MOCVD). The composition of two samples in our experiment were determined by X-ray photoelectron spectroscopy (XPS); the In content, lattice constants and crystal quality were measured by an X-ray diffraction (XRD) system (X-ray wavelength: 1.54056 nm); and the surface topography was measured by atomic force microscopy (AFM) and scanning electron microscopy (SEM).

2. Experimental procedure

The materials were grown by a VEECO MOCVD system with a 3×2 inch high speed rotating disk in a vertical gas-flow growth chamber. Figure 1 shows a schematic diagram of InAlN/GaN and InAlN/AlN heterostructures in this experiment. First, a 3 μm thick GaN template and a 1.5 μm thick AlN template were grown on the (002) sapphire substrate, respectively. During the GaN template growth, a 3 μm thick un-doped GaN template was grown at 1055 ℃ on a 30 nm thick low temperature GaN buffer layer, which was grown at 525 ℃ on the (002) sapphire substrate; during the AlN template growth, a 1.5 μm thick AlN template was grown at 1150 ℃ on a 30 nm thick low temperature AlN buffer layer, which was grown at 630 ℃ on the (002) sapphire substrate. Then, we grew InAlN epitaxial layers about 200 nm on the above GaN and AlN templates at 810 ℃ and 30 Torr. The thickness was estimated by an *in situ* layer reflection monitor. Trimethylgallium (TMGa), trimethylaluminum (TMAl), trimethylindium (TMIn) and ammonia (NH_3) were used as precursors for Ga, Al, In and N, respectively. H_2 was used as the carrier gas when growing GaN and AlN templates, while nitrogen (N_2) was used as the carrier gas when growing the InAlN epitaxial layer.

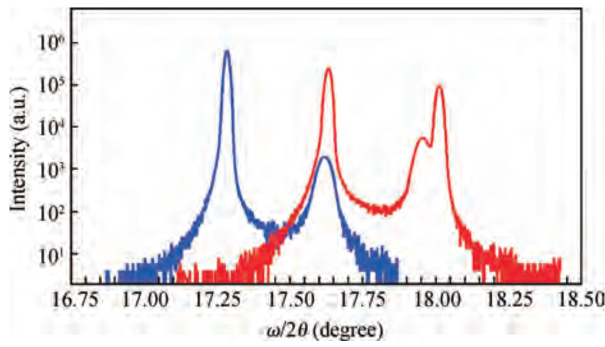

Fig. 3. $\omega/2\theta$ diffraction curves for (002) InAlN epilayers grown on GaN and AlN templates.

3. Results and discussion

Figure 2 shows near-surface XPS spectra for an InAlN epilayer grown on a GaN template. In Fig. 2, the penetration depth of the incident X-ray was approximately 8 to 9 nm. Before the measurement, a ~ 20 nm surface sample of InAlN epilayer was bombarded by an electron beam aiming to get a precise component result. From this figure, it is clear that the InAlN epilayer is a ternary alloy consisting of In, Al and N as primary components. Here, the oxygen and carbon, which are also found in XPS spectra, have been confirmed to be localized near the sample surface[16]. Element Ga also exists in the InAlN sample, but its content is extremly low, which does not affect the alloy component and properties and is generally negligible.

Structures consisting of ~ 200 nm InAlN/AlN (GaN) template/sapphire substrate were characterized by symmetric $\omega/2\theta$ X-ray diffraction (XRD) for GaN/AlN (002) reflection, and indium content in the InAlN epitaxial layer was determined by a $\omega/2\theta$ scan. Figure 3 shows the (002) XRD $\omega/2\theta$ scan for InAlN/GaN and InAlN/AlN samples. The spectrum is dominated by the GaN peak at an angle of 17.284° originating from the underlying GaN template, and by the AlN peak at an angle of 18.015° originating from the underlying AlN template. The InAlN epitaxial layer peaks are observed at 17.618° and 17.633° for samples grown on GaN and AlN templates, respectively, therefore the In content of the two samples is basically the same, and we only need to calculate one of them. Here, we chose the sample grown on a GaN template as a calculating example. The lattice parameter c can be directly calculated by the Bragg equation $c = l\lambda/(2\sin\theta)$[17], where l is the Miller index in (h, k, l) notation and θ is the Bragg angle. Along with parameter c, we can calculate lattice parameter a from asymmetric (105) reflection using the quadratic form of Bragg's equation given by[18]

$$\frac{1}{d_{hkl}^2} = \frac{4}{3}\frac{h^2 + k^2 + hk}{a^2} + \frac{l^2}{c^2}. \quad (1)$$

Assuming Vegard's law to hold $\mathrm{In}_x\mathrm{Al}_{1-x}\mathrm{N}$ and considering the biaxial strain in the layer, the indium content can be determined by applying the relation

$$x = -\frac{ac(1 + v_{(x)}) - ac_0^{\mathrm{AlN}} - a_0^{\mathrm{AlN}} c v_{(x)}}{ac_0^{\mathrm{AlN}} - ac_0^{\mathrm{InN}} - a_0^{\mathrm{InN}} c v_{(x)} + a_0^{\mathrm{AlN}} c v_{(x)}}, \quad (2)$$

where v is Poisson's ratio defined as $v = c_{13}/c_{33}$, and c_{13} and c_{33} are the elastic constants of the hexagonal III-nitrides.

Table 1. Comparison of XRD measurement results of two samples in this experiment.

	Template FWHM (002) (arcsec)	InAlN FWHM (002) (arcsec)	InAlN FWHM (102) (arcsec)
GaN template	204.9	3093	339.1
AlN template	84.12	282.3	313.5

The material constants used in this study are $a = 0.3111$ nm, $c = 0.498$ nm[19], $c_{13} = 99$ GPa, $c_{33} = 389$ GPa[20] for AlN; $a = 0.35378$ nm, $c = 0.57033$ nm[21], $c_{13} = 121$ GPa, $c_{33} = 182$ GPa[22] for InN. For the $\mathrm{In}_x\mathrm{Al}_{1-x}\mathrm{N}$ ternary alloy, both lattice constants and Poisson's ratio $v_{(x)}$ are obtained by linear interpolation from the values of binaries[23].

In Fig. 3, we can find two well-resolved InAlN peaks at 17.618° and 17.633°. With the parameters and formulas above, the In content was calculated to be ~ 16% in both cases. With this result, we can calculate the lattice dismatch $\Delta a/a$ to be ~ –0.26%, which corresponds to the nearly lattice matched condition because the lattice matched condition is determined by the lattice constant a along the a-axis of the wurtzite structure. Furthermore, there is no split InAlN peak for both samples. In addition, no other InAlN peaks exist in the wide-angle $\omega/2\theta$ scan results for InAlN epilayers grown on GaN and AlN templates, which are not shown here. Therefore, it is worth noting that the wurzite crystal structure of the InAlN epitaxial layer has no indication of phase separation between InN and AlN.

A comparison of additional XRD measurement results of two InAlN samples in this experiment is shown in Table 1. For the GaN template, its (002) FWHM value is 204.9″; for the AlN template, its (002) FWHM value is 84.12″. These results suggest that the two templates used in our experiment both have relatively high crystal quality. As we all know, the FWHM values for the (002) rocking curves could reflect the screw dislocation density, while the FWHM values for the (102) rocking curves reflect the edge dislocation density. The smaller these two values are, the better the crystal quality is. It is clear from Table 1 that the quality of the InAlN epitaxial layer grown on the AlN template is better than that grown on the GaN template. Therefore, a primary conclusion can be proposed that we could get a better InAlN epitaxial layer on a high quality AlN template than that on a high quality GaN template.

Figure 4 shows the typical AFM surface images of InAlN/GaN and InAlN/AlN heterostructures with a scan area of 5×5 $\mu\mathrm{m}^2$. The topography image of the InAlN epitaxial layer grown on a GaN template shows the presence of hillocks, pits and threadlike features on the surface. The average hillock diameter calculated is around 140 nm. These hillock-features are typical of MOCVD grown nitrides[24], and it is well known that the hillock size depends on the growth conditions (gas flow, growth temperature, etc.). Such defects have been reported to form close to the GaN/sapphire interface and may then propagate up to surface active layers[25], but this investigation is not complete. The root mean square (RMS) surface roughness for this sample was measured to be 0.592 nm, which is very low for the InAlN epitaxial layer, relatively. The topography image of the InAlN epitaxial layer grown on an AlN template,

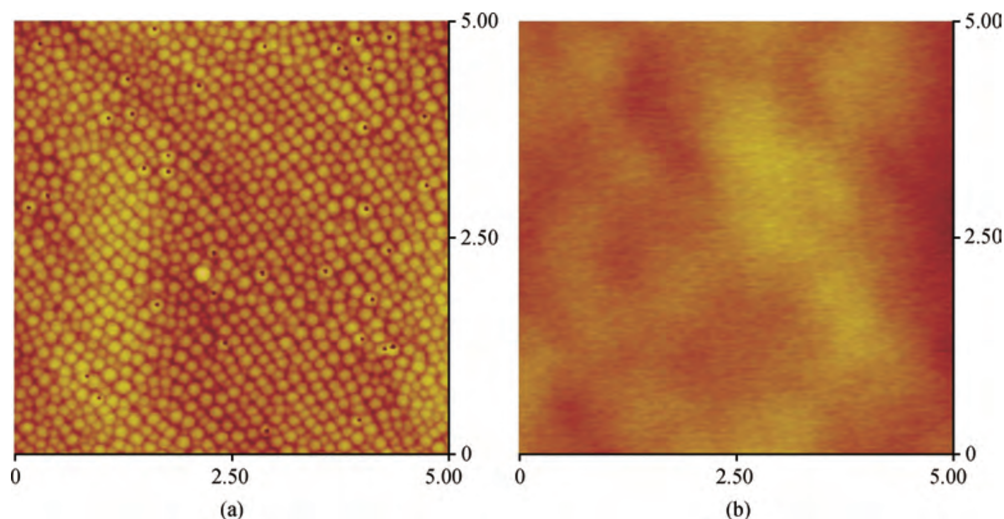

Fig. 4. AFM surface images of InAlN epitaxial layers grown on (a) GaN and (b) AlN templates, respectively.

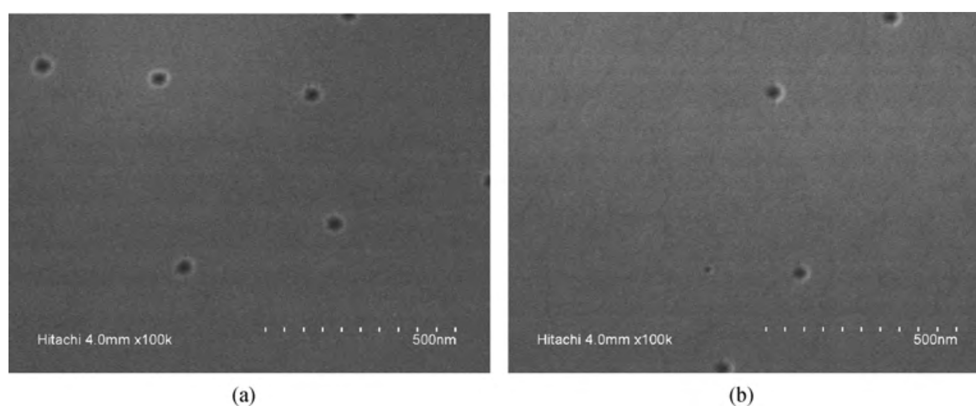

Fig. 5. SEM surface images of InAlN epitaxial layers grown on (a) GaN and (b) AlN templates, respectively.

however, presents a very smooth surface with an RMS value of 0.39 nm. Therefore, a lower pressure is needed for growing an InAlN epitaxial layer with better surface topography, because the mobility of Al atoms on the surface of the InAlN epitaxial layer becomes higher as the pressure decreases, which is beneficial for getting a smoother surface.

Figure 5 shows the SEM surface measurement results of InAlN epilayers grown on GaN (left) and AlN (right) templates, respectively. Both surfaces of the two samples in this experiment are very smooth, although it can be seen clearly that there are V-pits with a diameter of $\sim$ 35 nm on the InAlN epilayers grown on both templates. The V-pit densities are estimated as 4.2×10^8 cm^{-2} and 2.8×10^8 cm^{-2} for InAlN epilayers grown on the GaN and AlN templates, respectively (Fig. 4(a)).

According to the XRD, AFM and SEM measurement results presented above, such a primary conclusion can be summarized that the AlInN epitaxial layer grown on the AlN template has the same In content and a better surface topography, when compared to that grown on the GaN template under the same growth conditions. This is because the AlN template as the nucleation layer for InAlN growth has a lower dislocation density. Therefore, few threading dislocations are prolongated into the subsequent InAlN. Although the AlInN epilayer in our experiment is more lattice-matched with the GaN template, it is not the dominant factor but the dislocation density that determines the crystal quality of the InAlN epilayer. Therefore, the AlN template is a better choice than the GaN template for getting a high quality InAlN epilayer.

4. Conclusion

We grew InAlN epitaxial layers on high quality GaN and AlN templates, respectively, with the same growth parameters. The In content was measured to be $\sim$16% for both samples. For the InAlN epilayer grown on a GaN template, 309.3″ (002) FWHM, 339.1″ (102) FWHM, surface roughness of 0.593 nm and V-pit density of 4.2×10^8 cm^{-2} were achieved; for the InAlN epilayer grown on an AlN template, (002), (102) FWHM, surface roughness and V-pit density were 282.3″, 313.5″, 0.39 nm and 2.8×10^8 cm^{-2}, respectively. Therefore, a primary conclusion was proposed that both crystal quality and surface topography of the InAlN epilayer grown on the AlN template were better than that of the InAlN sample grown on the GaN template, which indicated that the AlN template is a better choice than the GaN template for achieving a high quality InAlN epilayer.

Acknowledgements

The authors would like to thank teacher Li Z P of Tsinghua University for the XPS measurements, Yuan X X, Shan G Q and Zhou Z C of the R&D Center for Semiconductor Lighting, Institute of Semiconductors, Chinese Academy of Sciences for XRD, AFM and SEM measurements, respectively.

References

[1] Khan M A, Shur M S, Kuznia J N, et al. Temperature activated conductance in GaN/AlGaN heterostructure field-effect transistors operating at temperatures up to 300-degrees-C. Appl Phys Lett, 1995, 66(9): 1083

[2] Ambacher O. Growth and applications of group III nitrides. J Phys D: Appl Phys, 1998, 31(20): 2653

[3] Nakamura S. The roles of structural imperfections in InGaN-based blue light-emitting diodes and laser diodes. Science, 1998, 281(5379): 956

[4] Wu Y F, Saxler A, Moore M, et al. 30-W/mm GaN HEMTs by field plate optimization. IEEE Electron Device Lett, 2004, 25(3): 117

[5] Carlin J F, Ilegems M. High-quality AlInN for high index contrast Bragg mirrors lattice matched to GaN. Appl Phys Lett, 2003, 83(4): 668

[6] Lorenz K, Franco N, Alves E, et al. Anomalous ion channeling in AlInN/GaN bilayers: determination of the strain state. Phys Rev Lett, 2006, 97(8): 085501

[7] Matsuoka T. Calculation of unstable mixing region in wurtzite $In_{1-x-y}Ga_xAl_yN$. Appl Phys Lett, 1997, 71(1): 105

[8] Dadgar A, Schulze F, Blasing J, et al. High-sheet-charge-carrier-density AlInN/GaN field-effect transistors on Si(111). Appl Phys Lett, 2004, 85(22): 5400

[9] Neuburger M, Zimmermann T, Kohn E, et al. Unstrained InAlN/GaN HEMT structure. Int J High Speed Electron Syst, 2004, 14(3): 785

[10] Dorsaz J, Carlin J F, Gradecak S, et al. Progress in AlInN–GaN Bragg reflectors: application to a microcavity light emitting diode. J Appl Phys, 2005, 97(8): 084505

[11] Feltin E, Butte R, Carlin J F, et al. Lattice-matched distributed Bragg reflectors for nitride-based vertical cavity surface emitting lasers. Electron Lett, 2005, 41(2): 94

[12] Akazawa M, Matsuyama T, Hashizume T, et al. Small valence-band offset of $In_{0.17}Al_{0.83}N$/GaN heterostructure grown by metal-organic vapor phase epitaxy. Appl Phys Lett, 2010, 96(13): 132104

[13] Choi S, Kim H J, Kim S S, et al. Improvement of peak quantum efficiency and efficiency droop in III-nitride visible light-emitting diodes with an InAlN electron-blocking layer. Appl Phys Lett, 2010, 96(22): 221105

[14] Fischer A M, Sun K W, Juday R, et al. Effect of growth temperature on the electron-blocking performance of InAlN layers in green emitting diodes. Appl Phys Express, 2010, 3(3): 031003

[15] Kim H J, Choi S, Kim S S, et al. Improvement of quantum efficiency by employing active-layer-friendly lattice-matched InAlN electron blocking layer in green light-emitting diodes. Appl Phys Lett, 2010, 96(10): 101102

[16] Miyoshi M, Kuraoka Y, Tanaka M, et al. Metalorganic chemical vapor deposition and material characterization of lattice-matched InAlN/GaN two-dimensional electron gas heterostructures. Appl Phys Express, 2008, 1(8): 081102

[17] Pereira S, Correia M R, Pereira E, et al. Interpretation of double X-ray diffraction peaks from InGaN layers. Appl Phys Lett, 2001, 79(10): 1432

[18] Angerer H, Brunner D, Freudenberg F, et al. Determination of the Al mole fraction and the band gap bowing of epitaxial $Al_xGa_{1-x}N$ films. Appl Phys Lett, 1997, 71(11): 1504

[19] Tanaka M, Nakahata S, Sogabe K, et al. Morphology and X-ray diffraction peak widths of aluminum nitride single crystals prepared by the sublimation method. Jpn J Appl Phys, Part 2, 1997, 36(8B): L1062

[20] Paszkowicz W, Cerny R, Krukowski S. Rietveld refinement for indium nitride in the 105–295 K range. Powder Diffr, 2003, 18(2): 114

[21] Paszkowicz W. X-ray powder diffraction data for indium nitride. Powder Diffr, 1999, 14(4): 258

[22] Wright A F. Elastic properties of zinc-blende and wurtzite AlN, GaN, and InN. J Appl Phys, 1997, 82(6): 2833

[23] Xue J S, Hao Y, Zhou X W, et al. High quality InAlN/GaN heterostructures grown on sapphire by pulsed metal organic chemical vapor deposition. J Cryst Growth, 2011, 314(1): 359

[24] Butte R, Carlin J F, Feltin E, et al. Current status of AlInN layers lattice-matched to GaN for photonics and electronics. J Phys D: Appl Phys, 2007, 40(20): 6328

[25] Vilalta-Clemente A, Poisson M A, Behmenburg H, et al. The structure of InAlN/GaN heterostructures for high electron mobility transistors. Phys Status Solidi A, 2010, 207(5): 1105